Supplementary information

Cross-immunity between strains explains the dynamical pattern of some paramyxoviruses

Samit Bhattacharyya; Per H. Gesteland; Kent Korgenski;
Ottar N. Bjørnstad; Frederick R. Adler

S1 Model

S1.1 Two-disease cross-immunity model

We extend a standard two-disease model to include partial cross-protective immunity between viruses [1, 2, 3, 4, 5]. Initially, individuals are susceptible to both viruses. Upon contracting one virus, they enter the infected class and become infectious. We assume both type of virus cannot simultaneously infect single individual host. After recovery, individuals acquire complete but temporary immunity against the original virus and partial temporary immunity against the second virus. After infection by both viruses, individuals are assumed to be transiently immune to both viruses.

The variables and related parameters for these two viruses (P and R) are described by corresponding subscripts. We assume that transmission is seasonally forced: $\alpha_i = \alpha_0(1 + \alpha_{00}\sin(2\pi(t-\phi)/T))$, $i = P$ and R, where α_0 and α_{00} are the virus-specific basic transmission rate and the seasonal amplitude, respectively (detailed description and values are given in table S1). The parameter ϕ represents the phase of the annual transmission cycle. Regular annual cycle may vary due to weather and climate conditions, assumed to be constant across years. We also assume that partial cross-immunity acts as reducing susceptibility to other pathogen. The complete model is given by:

$$\begin{aligned}
\frac{dS}{dt} &= \mu_0 N - \mu S - \frac{S}{N}\{\alpha_{_P} q_1[I_P + J_P] + \alpha_{_R} q_2[I_R + J_R]\} + \rho_{_P} R_P + \rho_{_R} R_R,\\
\frac{dI_P}{dt} &= \frac{\alpha_{_P} q_1 S}{N}[I_P + J_P] - \gamma_{_P} I_P - \mu I_P,\\
\frac{dI_R}{dt} &= \frac{\alpha_{_R} q_2 S}{N}[I_R + J_R] - \gamma_{_R} I_R - \mu I_R,
\end{aligned}$$

$$
\begin{aligned}
\frac{dR_P}{dt} &= \gamma_{_P} I_P - \frac{\alpha_{_R} q_2 \epsilon_{_R} R_P}{N}[I_R + J_R] - \rho_{_P} R_P + \rho_{_R} R - \mu R_P, \\
\frac{dR_R}{dt} &= \gamma_{_R} I_R - \frac{\alpha_{_P} q_1 \epsilon_{_P} R_R}{N}[I_P + J_P] - \rho_{_R} R_R + \rho_{_P} R - \mu R_R, \\
\frac{dJ_P}{dt} &= \frac{\alpha_{_P} q_1 \epsilon_{_P} R_R}{N}[I_P + J_P] - \gamma_{_P} J_P - \mu J_P, \\
\frac{dJ_R}{dt} &= \frac{\alpha_{_R} q_2 \epsilon_{_R} R_P}{N}[I_R + J_R] - \gamma_{_R} J_R - \mu J_R, \\
\frac{dR}{dt} &= \gamma_{_P} J_P + \gamma_{_R} J_R - \rho_{_P} R - \rho_{_R} R - \mu R, \qquad \text{(S1)}
\end{aligned}
$$

where S represents the susceptible population, I_P and I_R the infected populations, and R_P and R_R the population recovered from infection P and R respectively. Population J_P and J_R are infected by P and R, but immune to R and P respectively, and R is immune to both pathogen. The parameters ϵ_P and ϵ_R are the two parameters quantifies the strength of partial cross-protection from pathogens R and P respectively. The parameters γ_P, γ_R denote recovery rate from infection and, ρ_P, ρ_R denote the waning rate of immunity of pathogens P and R. A model schematic is given in the Figure S1(a).

S1.2 Two-disease competition model

The two-disease competition or convalescence model differs from the cross-immunity model in the mechanism by which the two pathogens interact. When clinical symptoms appear, individuals are quarantined at home or a health-care facility, with probability and duration dependent on the severity of disease, which we term the convalescent phase. During convalescence, they have a lower probability of exposure to and thus infection by other the virus, as described by the parameter θ (detailed in table S1). The complete model is given by

$$
\begin{aligned}
\frac{dS}{dt} &= \mu_0 N - \mu S - \frac{S}{N}\{\alpha_{_P} q_1 [I_P + J_P] + \alpha_{_R} q_2 [I_R + J_R]\} + \rho_{_P} S_P + \rho_{_R} S_R, \\
\frac{dI_P}{dt} &= \frac{\alpha_{_P} q_1 S}{N}[I_P + J_P] - \gamma_{_P} I_P - \mu I_P, \\
\frac{dI_R}{dt} &= \frac{\alpha_{_R} q_2 S}{N}[I_R + J_R] - \gamma_{_R} I_R - \mu I_R, \\
\frac{dC_P}{dt} &= \gamma_{_P} I_P - \delta_{_P} C_P - \frac{\alpha_{_R} q_2 \{\theta C_P\}}{N}[I_R + J_R] - \mu C_P, \\
\frac{dC_R}{dt} &= \gamma_{_R} I_R - \delta_{_R} C_R - \frac{\alpha_{_P} q_1 \{\theta C_R\}}{N}[I_P + J_P] - \mu C_R, \\
\frac{dS_P}{dt} &= \delta_{_R} C_R - \frac{\alpha_{_P} q_1 S_P}{N}[I_P + J_P] - \rho_{_P} S_P + \rho_{_P} R - \mu S_P,
\end{aligned}
$$

$$
\begin{aligned}
\frac{dS_R}{dt} &= \delta_{_P} C_{_P} - \frac{\alpha_{_R} q_2 S_R}{N}[I_R + J_R] - \rho_{_R} S_R + \rho_{_R} R - \mu S_R, \\
\frac{dJ_P}{dt} &= \frac{\alpha_{_P} q_1 S_P}{N}[I_P + J_P] + \frac{\alpha_{_P} q_1 \{\theta C_{_R}\}}{N}[I_P + J_P] - \gamma_{_P} J_P - \mu J_P, \\
\frac{dJ_R}{dt} &= \frac{\alpha_{_R} q_2 S_R}{N}[I_R + J_R] + \frac{\alpha_{_R} q_2 \{\theta C_{_P}\}}{N}[I_R + J_R] - \gamma_{_R} J_R - \mu J_R, \\
\frac{dR}{dt} &= \gamma_{_P} J_P + \gamma_{_R} J_R - \rho_{_P} R - \rho_{_R} R - \mu R, \qquad \text{(S2)}
\end{aligned}
$$

with notations matching the two-disease cross-immunity model. State variables C_P and C_R denote population that are convalescent post-infection by P and R respectively, and S_P and S_R represent those susceptible to pathogen P and R, but immune to R and P respectively. A model schematic is given in the Figure S1(b).

S1.3 Three-disease cross-immunity model

The three virus (P, R and Q) cross-immunity model is formulated in same way as the two-disease model. The variables have similar meaning as the two-disease cross-immunity model. The full model is given by

$$
\begin{aligned}
\frac{dS}{dt} &= \mu_0 N - \mu S - \frac{S}{N}\{\alpha_{_P} q_1 [I_P + J_P] + \alpha_{_R} q_2 [I_R + J_R] + \alpha_{_Q} q_3 [I_Q + J_Q]\} + \rho_{_P} R_P + \rho_{_R} R_R + \rho_{_Q} R_Q, \\
\frac{dI_P}{dt} &= \frac{\alpha_{_P} q_1 S}{N}[I_P + J_P] - \gamma_{_P} I_P - \mu I_P, \\
\frac{dI_R}{dt} &= \frac{\alpha_{_R} q_2 S}{N}[I_R + J_R] - \gamma_{_R} I_R - \mu I_R, \\
\frac{dI_Q}{dt} &= \frac{\alpha_{_Q} q_3 S}{N}[I_Q + J_Q] - \gamma_{_Q} I_Q - \mu I_Q, \\
\frac{dR_P}{dt} &= \gamma_{_P} I_P - \frac{R_P}{N}\{\alpha_{_R} q_2 \epsilon_{_{PR}} [I_R + J_R] + \alpha_{_Q} q_3 \epsilon_{_{PQ}} [I_Q + J_Q]\} - \rho_{_P} R_P + \rho_{_R} R - \mu R_P, \\
\frac{dR_R}{dt} &= \gamma_{_R} I_R - \frac{R_R}{N}\{\alpha_{_P} q_1 \epsilon_{_{RP}} [I_P + J_P] + \alpha_{_Q} q_3 \epsilon_{_{RQ}} [I_Q + J_Q]\} - \rho_{_R} R_R + \rho_{_P} R - \mu R_R, \\
\frac{dR_Q}{dt} &= \gamma_{_Q} I_R - \frac{R_Q}{N}\{\alpha_{_P} q_1 \epsilon_{_{QP}} [I_P + J_P] + \alpha_{_R} \epsilon_{_{QR}} [I_R + J_R]\} - \rho_{_Q} R_Q + \rho_{_Q} R - \mu R_Q, \\
\frac{dJ_P}{dt} &= \frac{\alpha_{_P} q_1 [I_P + J_P]}{N}\{\epsilon_{_{RP}} R_R + \epsilon_{_{QP}} R_Q\} - \gamma_{_P} J_P - \mu J_P, \\
\frac{dJ_R}{dt} &= \frac{\alpha_{_R} q_2 [I_R + J_R]}{N}\{\epsilon_{_{PR}} R_P + \epsilon_{_{QR}} R_Q\} - \gamma_{_R} J_R - \mu J_R, \\
\frac{dJ_Q}{dt} &= \frac{\alpha_{_Q} q_3 [I_Q + J_Q]}{N}\{\epsilon_{_{PQ}} R_P + \epsilon_{_{RQ}} R_R\} - \gamma_{_Q} J_Q - \mu J_Q,
\end{aligned}
$$

$$\frac{dR}{dt} = \gamma_P J_P + \gamma_R J_R + \gamma_Q J_Q - \rho_P R - \rho_R R - \rho_Q R - \mu R. \quad \text{(S3)}$$

The parameter ϵ_{ij}, $i, j = P, Q, R$ indicates the strength of cross-protection of pathogen i on pathogen j.

S2 Data analysis

We perform wavelet decomposition of the time series from the year 2002 to 2014 for all pathogens to disentangle periodicity in time-frequency space. Before wavelet decomposition, we add a unit vector to the time series and perform a log-transformation. We also perform cross-wavelet transform and wavelet coherence of pairs of time series to identify the phase difference between these time series in time-frequency space. All wavelet analysis are done using the Matlab package developed by Grinsted et al.(2004) [7].

S3 Baseline parameters, parameter estimation, likelihood profile and model selection methodology

We simulate the two-disease, three-disease and no-interaction models using baseline parameter values (table S1), and estimate transmission rate, seasonality, interaction parameters and the reporting probability for all three models using the time series data from the years 2002 to 2014. We set the population of Intermountain Health Care region including Greater Salt Lake City area at approximately 3 million, and also assume that the birth rate was 0.025 per year.

Model parameters were estimated by minimizing the negative log-likelihood. We calculate the likelihood that a chosen parameter set Θ explains the complete data $Y = y(t_1), y(t_2), ..., y(t_n)$, $n = 649$, within the confines of the process and observation models. This likelihood function $\mathcal{L}(\Theta)$ is a product of conditional likelihoods, $\mathcal{L}_{t_j}(\Theta)$, calculated at each time t_j for all 649 data points in time. We assume that the observed new infections (combined primary and secondary infections) each day follows a Poisson process with a mean of new infections predicted by the disease model. The log-likelihood function is:

$$\log \mathcal{L}(\Theta) = \sum_{j}^{n} \log \mathcal{L}_{t_j}(\Theta), \quad \text{(S4)}$$

where,

$$\log \mathcal{L}_{t_j}(\Theta) = \log \mathcal{L}_{t_j}(y(t_j)|\hat{y}_\Theta(t_j)) = y(t_j) \log \hat{y}_\Theta(t_j) - \log(y(t_j)!) - \hat{y}_\Theta(t_j), \quad \text{(S5)}$$

and $\hat{y}_{\Theta}(t_j)$ is observed new infections on day t_j as integrated output from disease and observation models.

We estimate the initial conditions of the ODE system and simulate each model exactly for 12 years to fit time series to the case reports (except hMPV which has approximately seven years of data). We estimate transmission, seasonality, interaction parameters and reporting probability.
As maximum likelihood estimates can be sensitive to the choice of initial values provided to the numerical optimization algorithm, we use a multiple starting point solver in Matlab (version R2013b) designed to identify the global optimum. We assume 50 different starting points, searching over the maximum range of possible values of each parameters. For each model, the solver was run for each of 50 different randomly drawn starting vectors (uniformly distributed pseudorandom numbers within bounds) for the unknown parameters. From this set of local maxima, the solution with the greatest likelihood was selected as the estimate for the global maximum.

To evaluate model parsimony, we use the Akaike Information Criterion (AIC)

$$AIC = -2\log(\mathcal{L}) + 2l, \tag{S6}$$

where l is the number of parameters in the model to be estimated, and $\mathcal{L}$ is the maximized value of the likelihood function for the estimated model. The model with the lowest AIC is considered the most parsimonious.

We use root mean squared error to calculate the mean deviance for error profile. Assuming our datasets to be distributed according to a Gaussian, minimizing the root mean squared error (RMSE) would be equivalent to maximizing the negative log-likelihood of the data. For each parameter set, we calculate RMSE from 10 sample model fit and average these to calculate the mean deviance.

S4 Sensitivity analysis

We use cross-validation approach to determine the confidence interval for the estimators. This involves partitioning the sample data into a *training set* and a *testing set*, where we perform the analysis on *training set* and validate the analysis on *testing set*. We perform multiple rounds (100 sample in each scenario) of cross-validation using different partitions (10%, 20% and 30%), and compute the 95% CI from these estimates for different parameters [8, 9].

References

[1] A. Camacho, S. Ballesteros, A. L. Graham, et al. *Explaining rapid reinfections in multiple-wave influenza outbreaks: Tristan da Cunha 1971 epidemic as a case study.* Proc. Roy. Soc. B: 278(1725) (2009), 3635-3643.

[2] F. B. Bang, *Epidemiological interference*. Int. J. Epid. 4 (1975), 337-342.

[3] M. Kamo and A. Sasaki, *The effect of cross-immunity and seasonal forcing in a multi-strain epidemic model*, Physica D 165 (2002), 228-241

[4] H.J. Wearing, P. Rohani *Ecological and immunological determinants of dengue epidemics*. Proc. Natl. Acad. Sci. USA 103 (2006), 11802-11807, .

[5] B. Adams, E. C. Holmes, C. Zhang, M. P. Mammen, Jr, S. Nimmannitya, S. Kalayanarooj, and M. Boots, *Cross-protective immunity can account for the alternating epidemic pattern of dengue virus serotypes circulating in Bangkok*, Proc. Nat. Acad. Sci., USA 103, (2006), 14234-14239.

[6] A.J. Arenas, G. Gonzlez, L. Jdar *Existence of periodic solutions in a model of respiratory syncytial virus RSV*, J. Math. Anal. Appl. 344 (2008), 969-980.

[7] A. Grinsted, J. C. Moore, J. C., & S. Jevrejeva *Application of the cross wavelet transform and wavelet coherence to geophysical time series. Nonlinear processes in geophysics*, 11(5/6) (2004), 561-566.

[8] R. Kohavi *A study of cross-validation and bootstrap for accuracy estimation and model selection". Proceedings of the Fourteenth International Joint Conference on Artificial Intelligence (San Mateo, CA: Morgan Kaufmann)* 2 (12) (1995), 1137-1143.

[9] S. Geisser *Predictive Inference*. New York, NY: Chapman and Hall. (1993), ISBN 0-412-03471-9.

Table S1: **Baseline parameter values (calibrated and taken from [6]) or range used in simulation**

Parameter	Epidemiological description	Values (or range)
μ_0	Host birth rate	0.025 year^{-1}
$1/\mu$	Life expectancy	70 years
α_{0P}	Transmission rate for virus P	3.5 week^{-1}
α_{00P}	Seasonal amplitude for virus P	0.4
α_{0R}	Transmission rate for virus R	3.5 week^{-1}
α_{00R}	Seasonal amplitude for virus R	0.4
$q_i, (i = 1, 2, 3)$	Transmission probability	0.5
$1/\gamma_P$	Average infectious period for virus P	10 days
$1/\gamma_R$	average infectious period for virus R	10 days
ϵ_P	Strength of cross-protection of R for virus P	[0,1]
ϵ_R	Strength of cross-protection of P for virus R	[0,1]
$1/\delta_P$	Average convalescence period for virus P	30 days
$1/\delta_R$	Average convalescence period for virus R	30 days
$1/\rho_P$	Average waning period for virus P	1 year
$1/\rho_R$	Average waning period for virus R	1 year
θ	Strength of convalescence	[0,1]

Table S2: **Parameter estimation from single disease SIR model, two-disease cross-immunity model (S2) and convalescence model (S3) (in same units as in table S1)**

Disease	Transmission rate	Seasonal amplitude	Phase	Interaction	Reporting probability	Goodness-of-fit	AIC
Single SIR model							
RSV	1.4001	0.27	34.4	-	0.02	0.4365	2.7×10^4
HPIV-1	1.5	0.24	22.39	-	0.0025	-0.1064	1.9948×10^4
HPIV-2	1.8	0.18	35.41	-	0.0017	-0.3345	1.154×10^4
HPIV-3	1.89	0.21	5.9736	-	0.0037	0.0664	1.5636×10^4
Cross-immunity model							
RSV - HPIV-1	(3.4,2.9)	(0.4,0.33)	(-17.5,-29.5)	(0.9,0.54)	(0.018,0.0012)	(0.35,0.47)	2.36×10^4
RSV - HPIV-2	(3.3,2.5)	(0.4,0.28)	(-17.99,-20.001)	(0.9,0.796)	(0.018, 0.0007)	(0.49,0.23)	2.0823×10^4
RSV - HPIV-3	(3.4,2.0)	(0.4,0.31)	(-18.0,-11.0)	(0.87,0.63)	(0.018,0.016)	(0.3,0.134)	2.2186×10^4
RSV - hMPV	(3.4,3.9)	(0.4,0.3)	(0.005,4.99)	(0.92,0.45)	(0.018,0.009)	(0.63,0.40)	1.3369×10^3
Convalescence model							
RSV - HPIV-1	(3.4,2.1)	(0.4,0.39)	(-17.99,-25.0)	0.8001	(0.02,0.0045)	(0.32,-1.78)	2.41×10^4
RSV - HPIV-2	(3.4,2.8)	(0.4,0.35)	(-18.99,-21.99)	0.55	(0.018, 0.001)	(0.23,-0.16)	2.1529×10^4
RSV - HPIV-3	(3.4,3)	(0.4,0.3)	(-18.0,-6.99)	0.1	(0.02,0.0018)	(0.4308,0.07)	2.437×10^4

Table S3: **Parameter estimates for the three-disease cross-immunity model (RSV - HPIV-1 - HPIV-2) (in same units as in table S1)**

Transmission rate	Seasonal amp	Phase	Interaction $(\epsilon_{PQ}, \epsilon_{QP}; \epsilon_{PR}, \epsilon_{RP}; \epsilon_{RQ}, \epsilon_{QR})$	Reporting probabiliy	Goodness-of-fit	AIC
(3.2,3.1,2.5)	(0.4,0.45,0.3)	(-17, -36, -27)	(0.75,0.8;0.32,0.9;0.95,0.9)	(0.025,0.0018,0.0007)	(0.43,0.47,0.328)	2.81×10^4

Table S4: **Parameter estimation from single disease SIR model with relaxing the period of immunity (in same units as in table S1)**

Disease	Transmission rate	Seasonal amplitude	Phase	Immunity (yrs)	Reporting probability	Goodness-of-fit	AIC
HPIV-1	1.8	0.2	-34.9	8.74	0.01	0.4385	1.4319×10^4
HPIV-2	1.8	0.19	-30.9	5.82	0.005	0.3361	1.4085×10^4
HPIV-3	1.7	0.26	-5	1.7018	0.0037	0.0219	2.4055×10^4

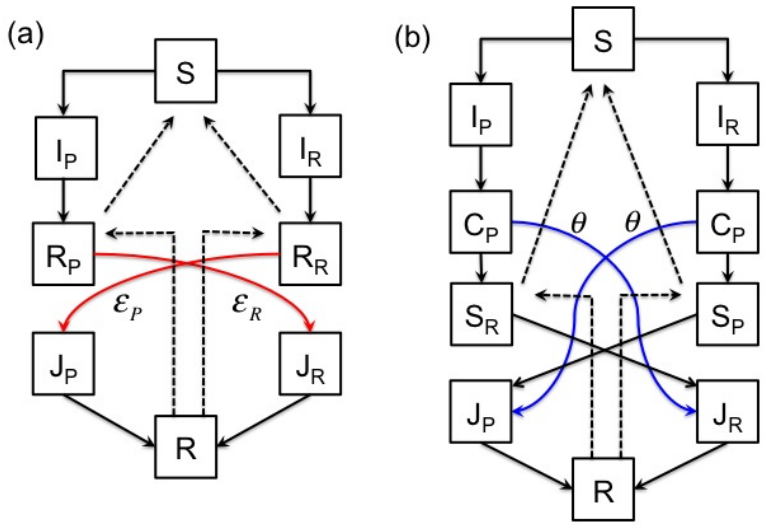

Figure S1: **Schematic of (a) cross-immunity and (b) competition model.** The black solid arrow denotes usual disease transmission, and dotted arrows represents waning of immunity. The colored arrows (red in (a) and blue in (b)) indicate the interaction by cross-immunity and convalescence.

Table S5: **Confidence interval of estimated parameters of two-disease cross-immunity model (in same units as in table S1)**

Parameters	Pathogen	10% partition	20% partition	30% partition
Transmission rate	RSV	(2.8, 4.04)	(2.7, 4.14)	(2.64, 4.12)
	HPIV-1	(2.9, 3.2)	(2.8, 3.2)	(2.7, 3.19)
Seasonal amp	RSV	(0.36, 0.43)	(0.35, 0.43)	(0.35, 0.438)
	HPIV-1	(0.247, 0.36)	(0.238, 0.36)	(0.238, 0.377)
Phase	RSV	(-18.9, -16.4)	(-18.9, -16.5)	(-18.9, -16.09)
	HPIV-1	(-31.2, -27.93)	(-31.47, -28.1)	(-31.70, -27.62)
Interaction	RSV	(0.862, 0.927)	(0.858, 0.93)	(0.833, 0.936)
	HPIV-1	(0.493, 0.586)	(0.484, 0.587)	(0.463, 0.604)
reporting probability	RSV	(0.0143, 0.0254)	(0.0124, 0.0278)	(0.0109, 0.0295)
	HPIV-1	(0.0011, 0.0014)	(0.0011, 0.0031)	(0.001, 0.0034)
Transmission rate	RSV	(2.84, 3.84)	(2.63, 4.05)	(2.58, 4.02)
	HPIV-2	(2.309 , 2.97)	(2.306, 2.78)	(2.308, 2.78)
Seasonal amp	RSV	(0.37, 0.427)	(0.35, 0.429)	(0.35, 0.442)
	HPIV-2	(0.194, 0.305)	(0.174, 0.31)	(0.185, 0.3216)
Phase	RSV	(-19.38, -17.02)	(-19.57, -16.94)	(-19.66, -16.57)
	HPIV-2	(-21.483, -18.70)	(-22.21, -18.456)	(-22.36, -18.25)
Interaction	RSV	(0.869, 0.92)	(0.853, 0.93)	(0.842, 0.94)
	HPIV-2	(0.758, 0.829)	(0.761, 0.849)	(0.74, 0.86)
reporting probability	RSV	(0.0142, 0.0237)	(0.0131, 0.0258)	(0.0108, 0.0285)
	HPIV-2	(0.0006, 0.0008)	(0.0006, 0.0017)	(0.0004, 0.0018)
Transmission rate	RSV	(2.923, 3.97)	(2.78, 4.056)	(2.6, 4.148)
	HPIV-3	(1.95, 2.09)	(1.9, 2.19)	(1.9 2.2)
Seasonal amp	RSV	(0.372, 0.426)	(0.35, 0.436)	(0.35, 0.448)
	HPIV-3	(0.214, 0.324)	(0.195, 0.328)	(0.1935, 0.3411)
Phase	RSV	(-19.27, -16.89)	(-19.48, -16.87)	(-19.71, -16.87)
	HPIV-3	(-12.64, -9.893)	(-12.91, -9.49)	(-13.42, -9.26)
Interaction	RSV	(0.834, 0.89)	(0.826, 0.91)	(0.806, 0.913)
	HPIV-3	(0.582, 0.676)	(0.586, 0.679)	(0.567, 0.692)
reporting probabiltiy	RSV	(0.0133, 0.025)	(0.0132, 0.0263)	(0.0113, 0.0292)
	HPIV-3	(0.0102, 0.0246)	(0.0092, 0.0259)	(0.0082, 0.0293)
Transmission rate	RSV	(3.35, 3.89)	(3.23, 3.98)	(3.13, 4.01)
	hMPV	(3.8, 3.99)	(3.775, 4.02)	(3.76, 4.036)
Seasonal amp	RSV	(0.374, 0.425)	(0.37, 0.432)	(0.368, 0.431)
	hMPV	(0.291, 0.309)	(0.2904, 0.314)	(0.2902, 0.3139)
Phase	RSV	(-0.457, 0.535)	(-0.628, 0.657)	(-0.718, 0.744)
	hMPV	(4.32, 5.539)	(4.40, 5.6)	(4.42, 5.758)
Interaction	RSV	(0.92, 0.93)	(0.90, 0.94)	(0.88, 0.96)
	hMPV	(0.45, 0.46)	(0.43, 0.48)	(0.41, 0.48)
reporting probability	RSV	(0.0155, 0.022)	(0.0144, 0.0236)	(0.0125, 0.0266)
	hMPV	(0.0087, 0.0095)	(0.0086, 0.0097)	(0.0089, 0.0098)

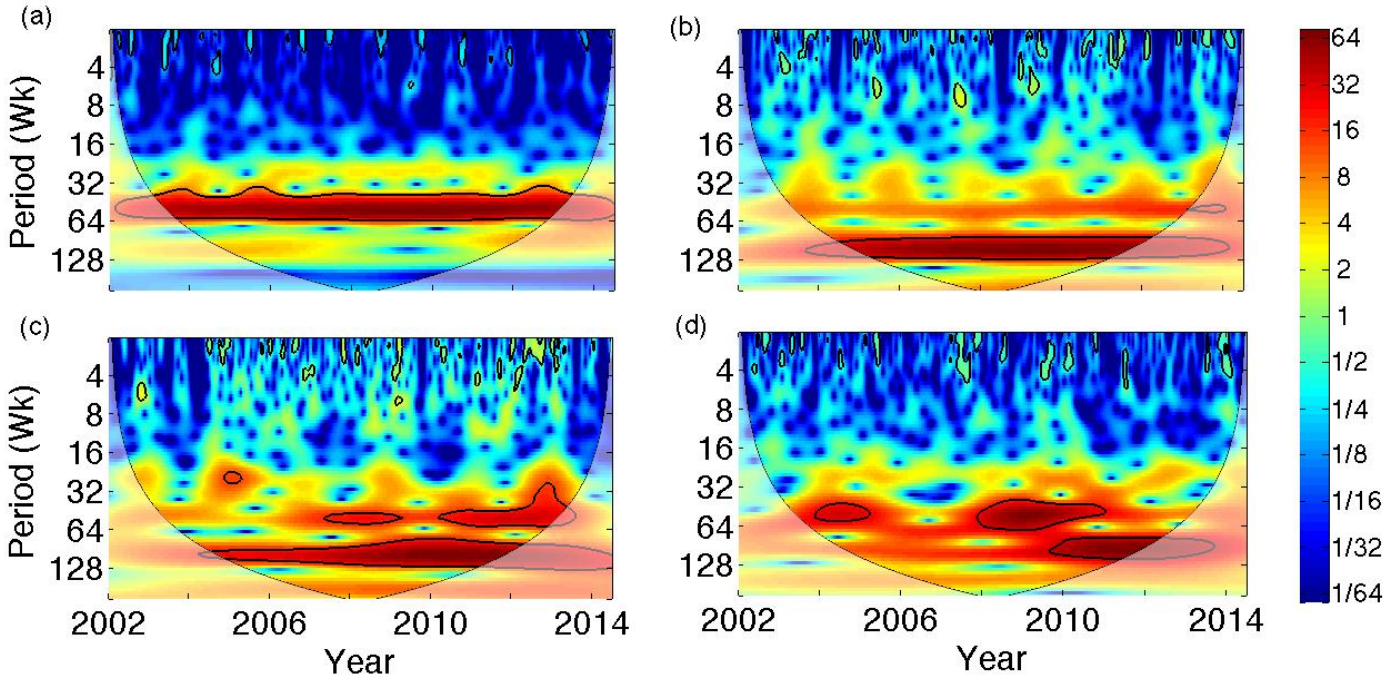

Figure S2: **Continuous wavelet transformation (CWT) of log-transformed reports: (a) RSV, (b) HPIV-1, (c) HPIV-2, (d) HPIV-3.** The 5% significance level against red noise is shown as a thick contour indicating stronger support for cycles of the period identified on the left axis. Other black line denotes the cone of influence (COI), and the region where edge effects might distort the picture is shown in a lighter shade.

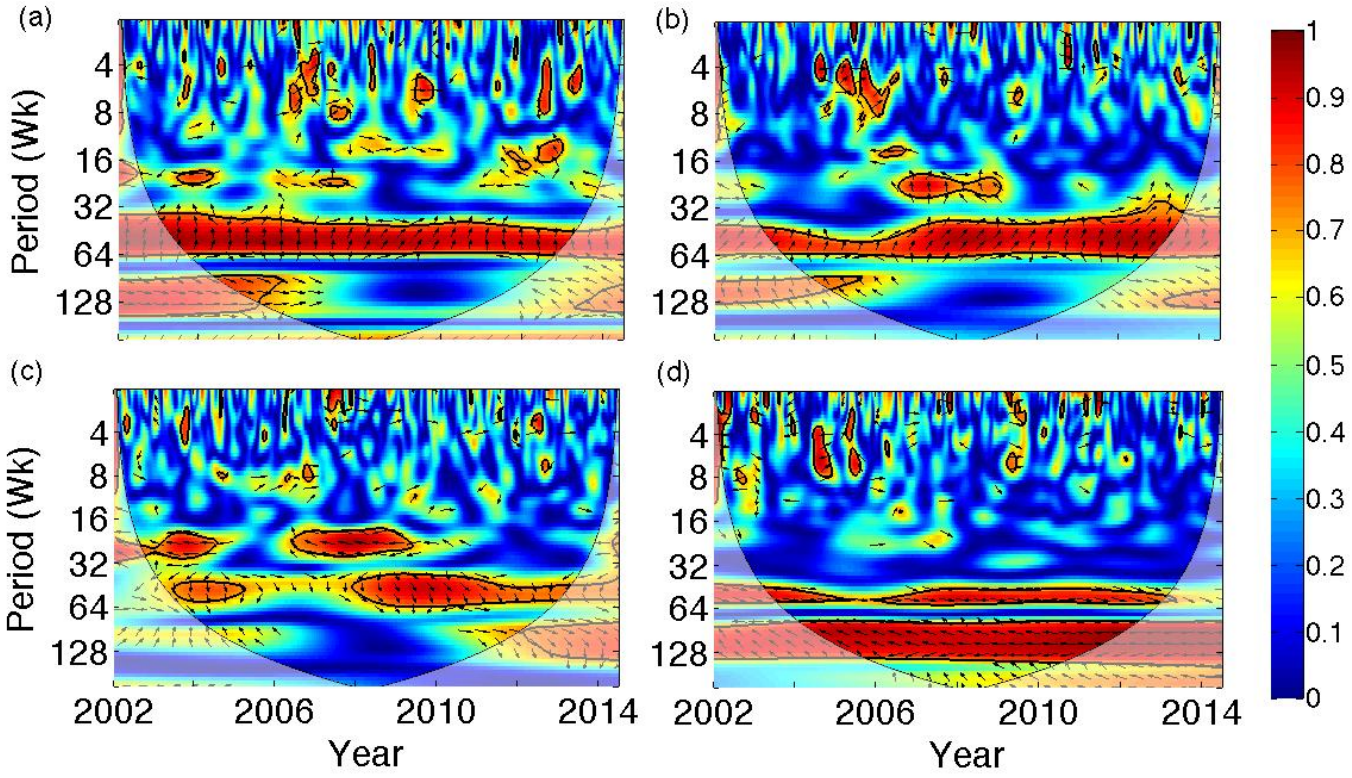

Figure S3: **Wavelet coherence between pair of the time series (a) RSV - HPIV-1, (b) RSV - HPIV-2, (c) RSV - HPIV-3, (d) HPIV-1 - HPIV-2.** The 5% significance level against red noise is shown as a thick contour. The direction of arrows in significant sections shows phase behavior of the two time series. (In-phase pointing right, anti-phase pointing left, down pointing time series 1 leading time series 2, and up pointing time series 2 leading time series 1). For example, (a) HPIV-1 is leading or in-phase with RSV in most of the time period, (b) HPIV-2 leading or in-phase with RSV, (c) RSV is leading or in anti-phase with HPIV-3, and (d) HPIV-1 and HPIV-2 are completely out of phase over a large region.

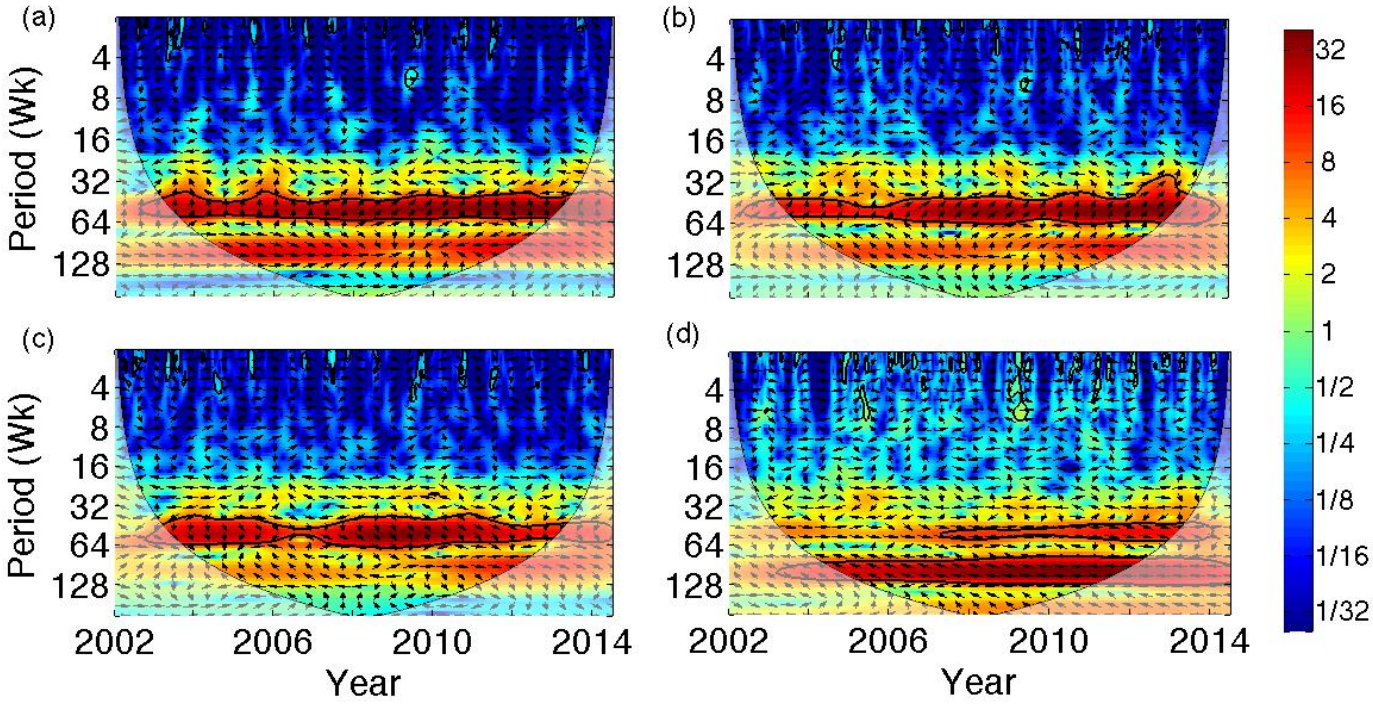

Figure S4: **Cross wavelet transform (XWT) between pair of the time series (a) RSV - HPIV-1, (b) RSV - HPIV-2, (c) RSV - HPIV-3, (d) HPIV-1 - HPIV-2.** The 5% significance level against red noise is shown as a thick contour. Arrows have similar interpretation as in Figure S3.

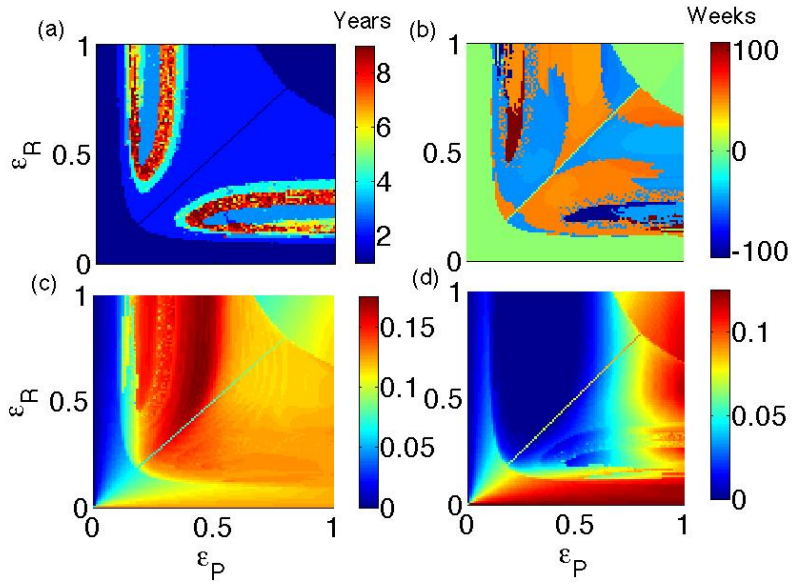

Figure S5: **Dynamical consequences of varying strength of cross-protection in two-disease cross-immunity model (S1) with base line parameter values (Table S1):** (a) period of attractors, (b) phase difference, (c) maximum peak size, and (d) minimum peak size in last 10 years of simulation.

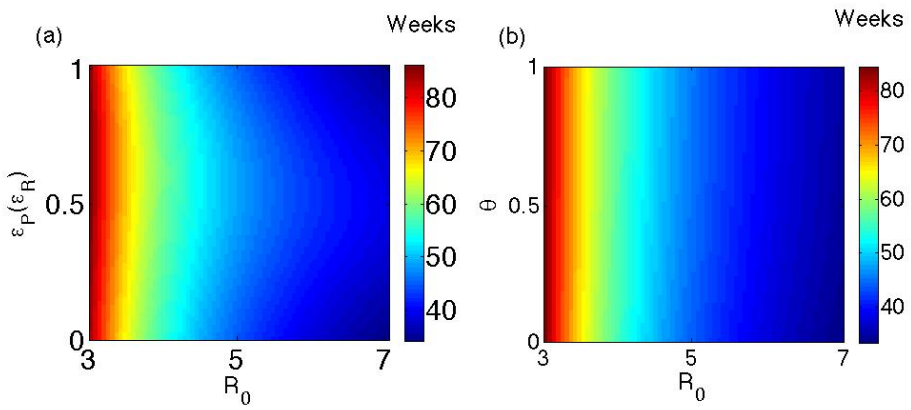

Figure S6: **Inter-epidemic period due to varying strength of interaction and R_0:** (a) two disease cross-immunity model (S1), (b) convalescence model (S2). The parameters values are baseline values as given in table S1.

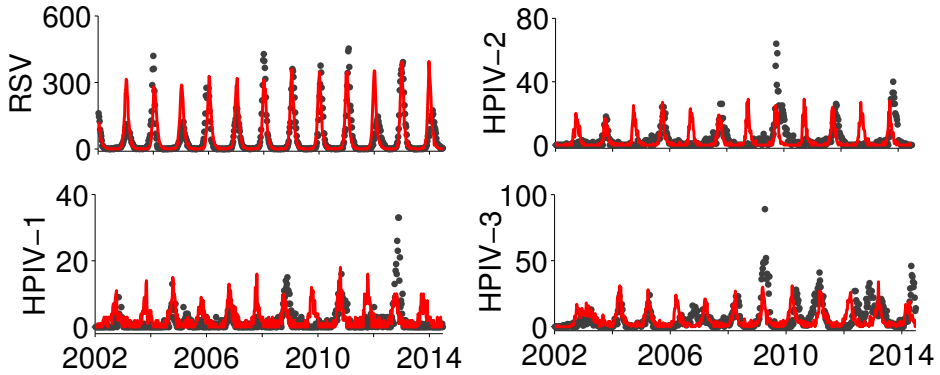

Figure S7: **Fitting results of single SIR model to RSV and three HPIV assuming immunity wanes in one year.** The black dots denote the data and red line is the model fit. The no-interaction model can explain the annual epidemic pattern of RSV, but it can not explain the biennial pattern of HPIV-1 and HPIV-2.

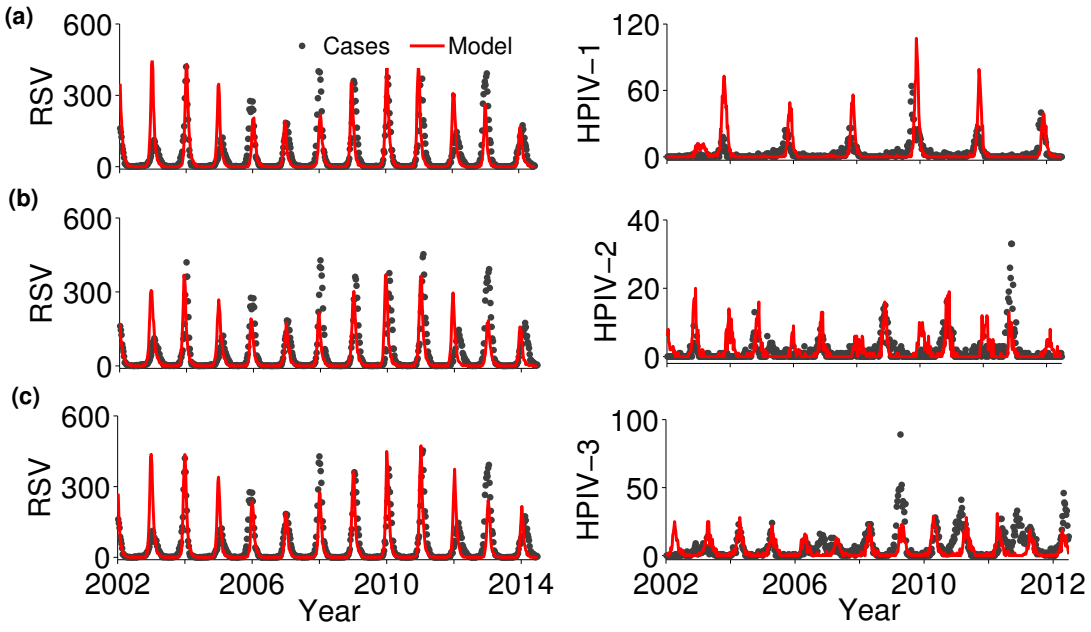

Figure S8: **Pairwise (horizontal panel) fitting results of two-disease competition model to RSV and with each of HPIV serotypes.** Although, the two-disease competition model captures the RSV - HPIV-1 dynamics, it provides a poor fit to the RSV - HPIV-2.

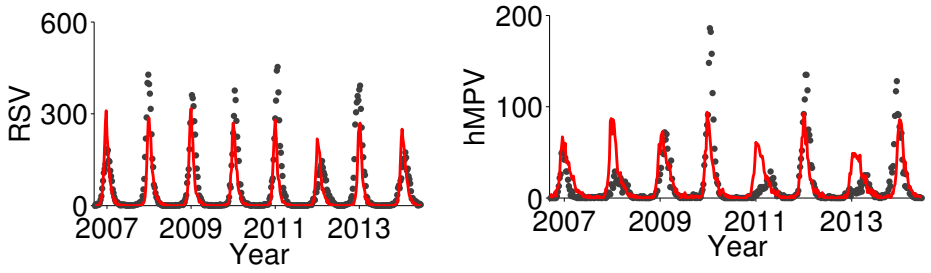

Figure S9: **Fitting results of two-disease cross-immunity model to the RSV and hMPV.** The black dots denote the data and red line is the model fit. Two-disease cross-immunity model can capture the annual cycle of RSV and hMPV.

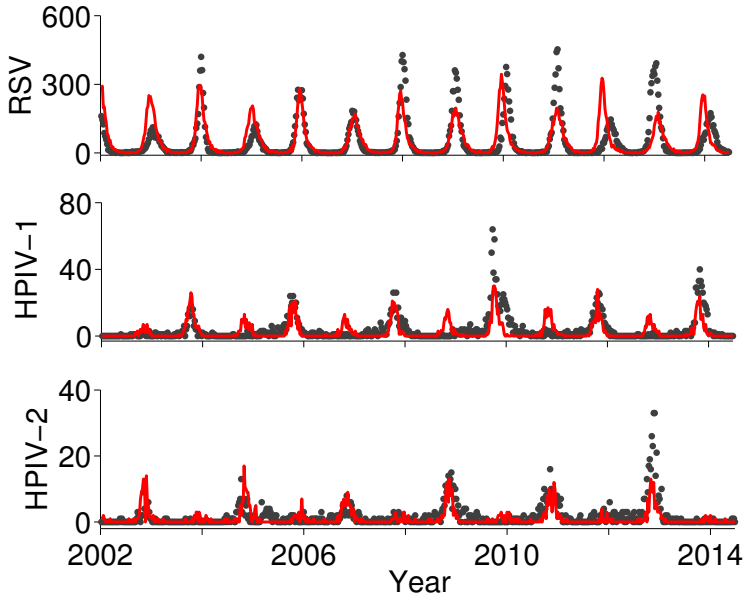

Figure S10: **Fitting results of three-disease cross-immunity model to RSV, HPIV-1 and HPIV-2.** The black dots denote the data and red line is the model fit. Three-disease model does not improve the fit to the data compared to the two-disease cross-immunity model.

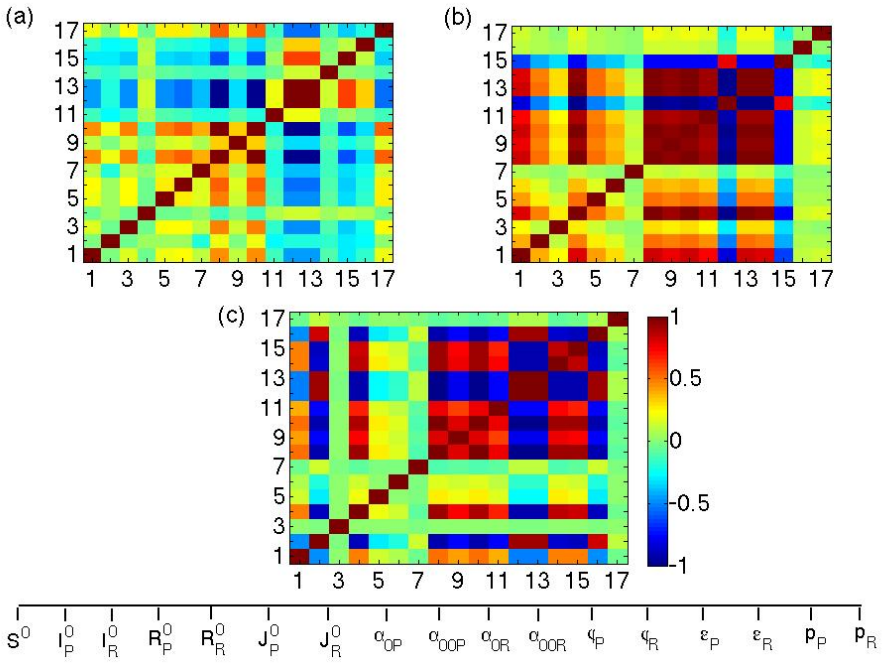

Figure S11: **Correlation matrix of estimated parameters (including ICs) of two-disease cross-immunity model.** (a) RSV - HPIV-1, (b) RSV - HPIV-2, and (c) RSV - HPIV-3. The axis label is described below. The first seven ticks represents the seven variables of ODE system, and the next ten ticks are model parameters. All matrices are scaled to [-1,1]. In RSV - HPIV-1 estimation, α_{0R} is strongly positively correlated with α_{0P}, but negatively correlated with phase (offset parameter) of the two pathogens. In RSV - HPIV-2, RSV - HPIV-3, there are relatively high correlation (positive or negative) among model parameters. The seasonal offset parameters ϕ_P and ϕ_R of annual epidemic cycle of RSV and HPIV-3 are strongly negatively correlated with other parameters. In both case, the interaction parameter has negative correlation with offset parameter. In RSV - HPIV-3, the initial conditions (I_P^0 and R_P^0) are also strongly correlated with most of model parameters.

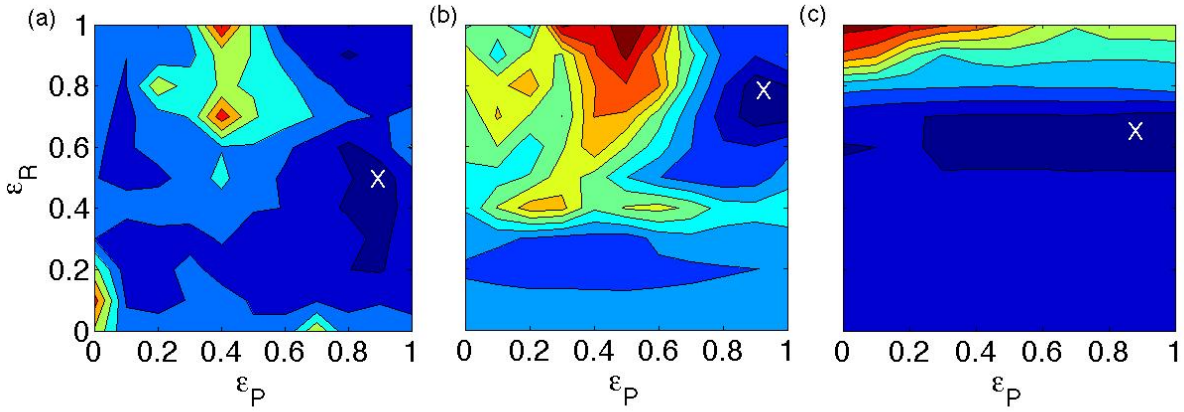

Figure S12: **Error profile in parameter estimation of two-disease cross-immunity model (ref. Figure 2, main text).** (a) RSV - HPIV-1, (b) RSV - HPIV-2, and (c) RSV - HPIV-3. The color against pair of parameter values represents the mean deviance between data and model output from 10 sample model fit (with red to blue represent highest to lowest deviance). The white 'X' in the figure indicates the best estimates of parameters (ϵ_P, ϵ_R) in the two-disease cross-immunity model fit (table S1).

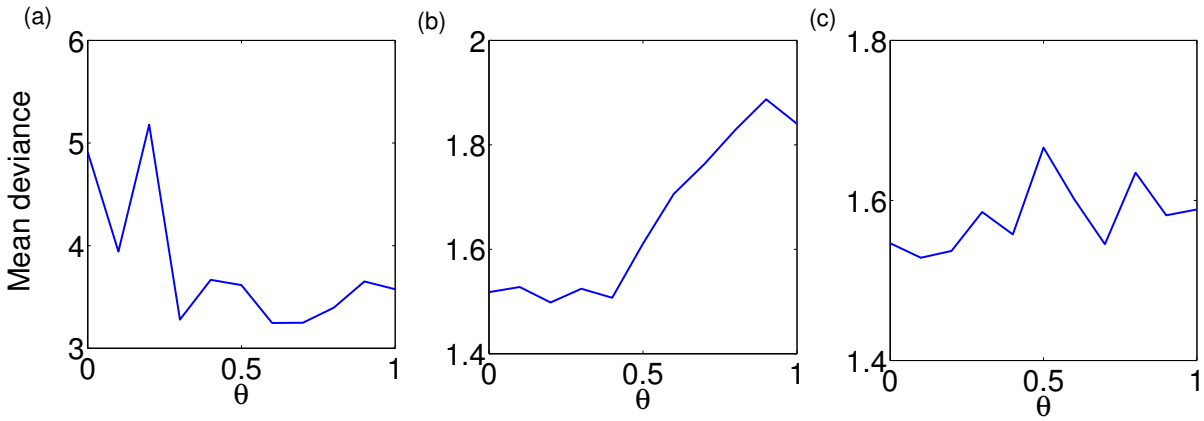

Figure S13: **Error profile in two-disease competition model fit (ref. Figure S8).** (a) RSV - HPIV-1, (b) RSV - HPIV-2, and (c) RSV - HPIV-3. The vertical axis gives the mean deviance of 10 sample model fit.

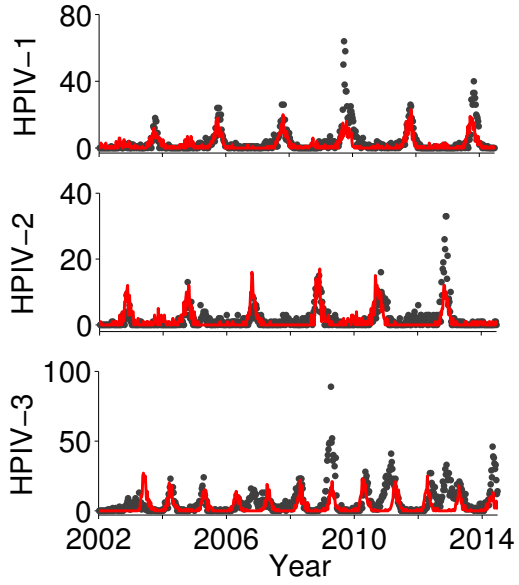

Figure S14: **Estimating waning immunity by fitting single SIR model to three HPIV serotypes datasets.** The no-interaction model explains the biennial epidemic pattern of HPIV-1 and HPIV-2, and annual epidemic pattern for HPIV-3 for different values of waning immunity. See text for more discussion.

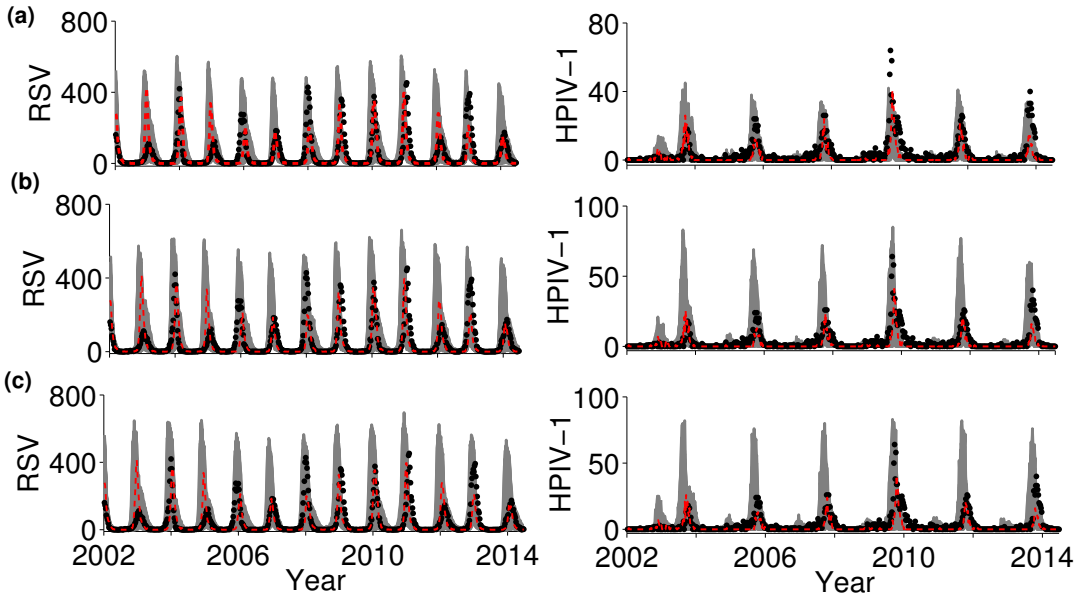

Figure S15: **Generalised cross validation analysis of RSV and HPIV-1.** Each horizontal panel denote plots with (a) 90%, (b)80% and (c) 70% training set obtained from entire dataset. The gray lines are 100 samples in each case. Red dotted line is the original fit and black dots denote the cases.

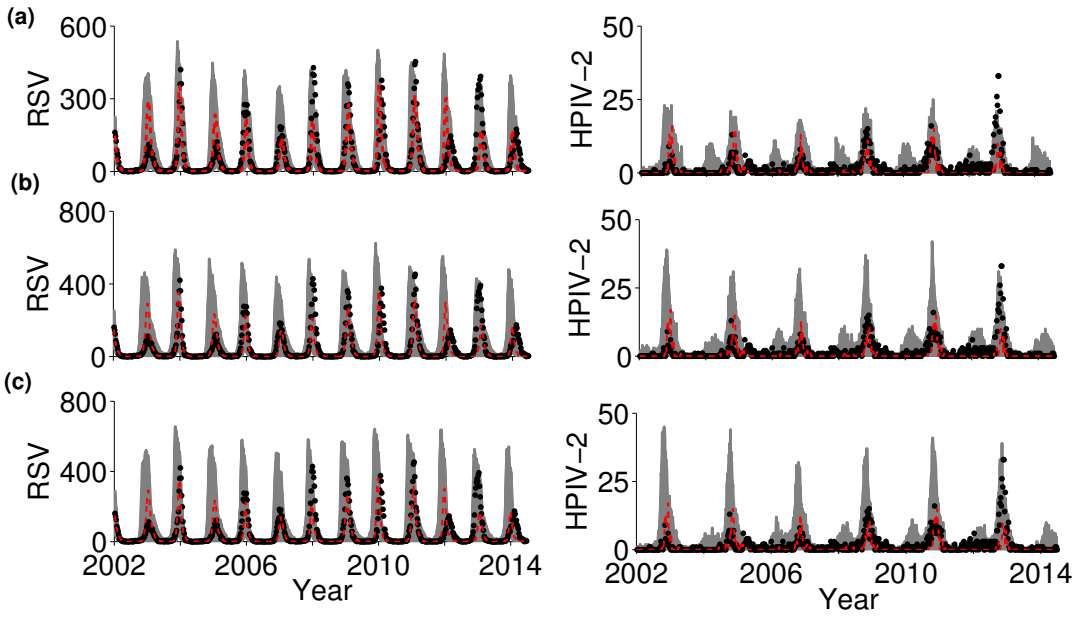

Figure S16: **Generalised cross validation analysis of RSV and HPIV-2.** Notation as in Figure S15.

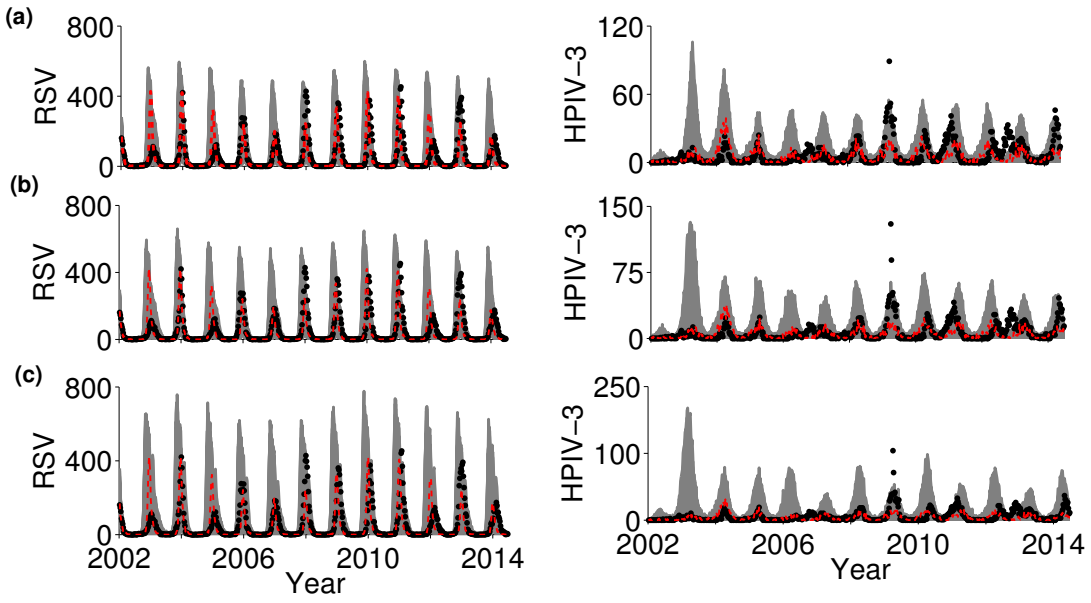

Figure S17: **Generalised cross validation analysis of RSV and HPIV-3.** Notation as in Figure S15.

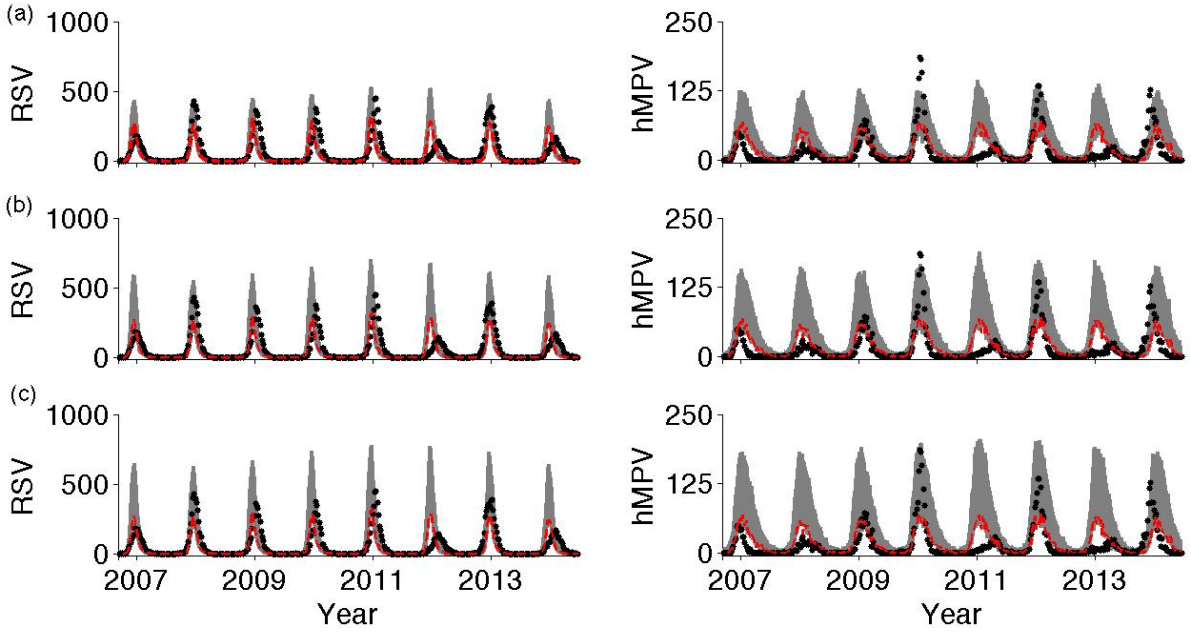

Figure S18: **Generalised cross validation analysis of RSV and hMPV.** Notation as in Figure S15.